Math. Scientist **13**, 135–151 (1988)
Printed in England

MATHEMATICAL APPROACHES TO MODELLING THE OCULOMOTOR CONTROL SYSTEM

R. C. FRECKER* AND W. J. MACLEAN**, *University of Toronto*

Abstract

Study of the eye-movement (oculomotor) control system provides insight into the functioning of motor systems in general and presents a means of understanding the diverse control strategies employed by the brain. This paper discusses the concept of modelling with particular emphasis on the oculomotor system. Mathematical techniques derived from engineering control systems theory are considered as they pertain to oculomotor modelling.

EYE MOVEMENT; SACCADE; MATHEMATICAL MODELLING

1. Introduction

Vision is one of man's richest sources of information. Further, the ability to move one's eyes in a coordinated fashion enhances the ability of the visual system by reducing the need for head motion, stabilizing the visual platform, and enhancing stereoscopic vision through coordinated fixation of both eyes on objects of interest.

The oculomotor (eye-movement) system comprises the various structural and functional components which permit the direction of gaze to be adjusted to meet the requirements of day-to-day activity. Its elements include six muscles attached to the outside of each eye, the nerves which conduct signals to and from these muscles, and the higher centers which process these signals. The oculomotor control system is the aggregate of information-processing elements which are integrated to provide an optimal relationship between eye position and the demands of a current task. To better understand the function of this control system it is helpful to be able to relate input and output functions quantitatively and to build mathematical models which take into account a wide range of relevant control parameters, error signals and a variety of system disturbances. Certain mathematical techniques have proved especially useful in modelling the oculomotor control system.

This paper briefly describes the oculomotor system, gives a rationale for modelling it, and discusses various modelling approaches. It then discusses a number of mathematical tools which are used for building oculomotor models and concludes by briefly speculating on the techniques which seem most likely to advance the field.

Received 4 May 1988.
*Institute of Biomedical Engineering and **Department of Electrical Engineering, University of Toronto, Ont, Canada M5S 1A4.

2. The oculomotor system

The eyeball is an approximately spherical globe, about an inch in diameter, which is housed in a bony socket in the skull (the orbit). The orbit is lined with fat to stabilize the eyeball and facilitate its movement (Figures 1(a), 1(b)).

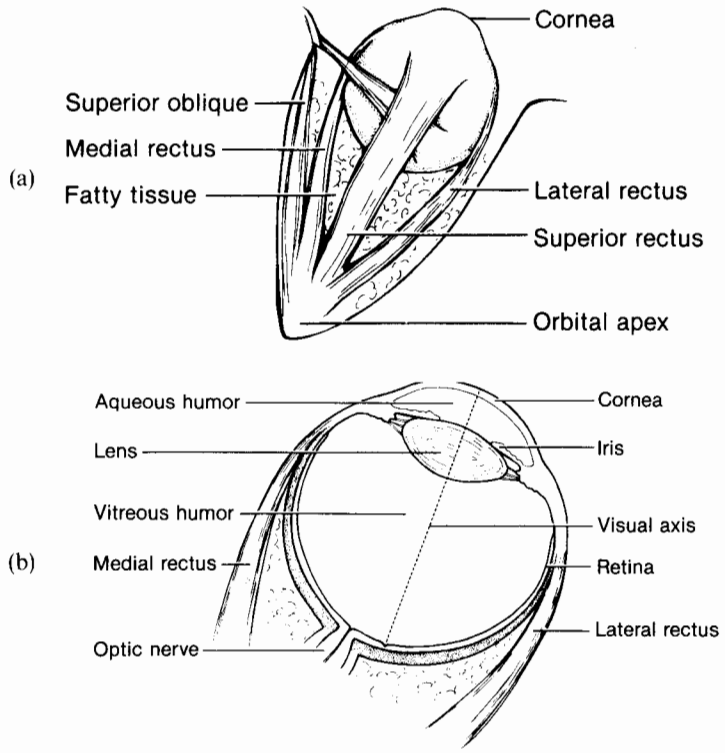

Figure 1. Anatomy of the oculomotor 'plant'. (a) View of globe from above showing muscle attachments to orbital apex. (b) A schematic representation of the eye showing the main intraocular elements.

The globe contains various elements which act together to form an image of external visual reality on a multi-element photodetector matrix—the *retina*. The *cornea* is a high-power fixed refractive element, while the lower-powered *lens* is capable of adjusting its dioptric strength to bring objects at various distances into focus on the retina. The *iris diaphragm* in front of the lens varies the size of its central *pupil* in response to changing levels of brightness. A large body of gel behind the lens (the *vitreous humor*) offers mechanical support to the lens and shape to the eyeball. The liquid in which the iris exists (the *aqueous humor*) is under slight pressure and also serves to maintain the sphericity of the globe.

The myriad photodetector cells of the retina are responsible for color and high spatial acuity vision (*cones*) and low-light-level (black and white) vision and motion detection (*rods*). Both these cell types transduce light into minute electrical signals through the interactions of photons with complex cellular

molecules which, on absorbing photon energy, change shape. Color, intensity and motion signals are preprocessed in the retina and then transmitted as coded images along the 1000000 nerve fibres of each *optic nerve* to the brain's *visual cortex*. In the central region of the retina is an area of densely packed cells, primarily cones, called the *fovea*. Since this region has a very high density of receptors it can better resolve spatial detail, and is therefore the preferred position on the retina for the image of an object of regard. An imaginary line drawn through the center of the pupil to the fovea is referred to as the axis of foveation, or the *line of sight*.

Attached to the outside of each globe are six *extraocular muscles* which, by coordinated contraction and relaxation, rotate the eye around three orthogonal axes. Motion in the plane perpendicular to the line of sight predominates. The moment of inertia of the globe is small compared with the forces generated by the muscles moving it and movement of the fluid within the globe is considered negligible in determining its moment of inertia (Robinson, (1981)). The lateral and medial recti (Figure 1) move the eye horizontally; vertical movements are generated by the superior and inferior recti and the superior and inferior obliques. The neuronal signals which drive these muscles arise in different areas of the brain.

The globe, the extraocular muscles and the orbital tissues are known collectively as the *oculomotor plant*. The input to this plant comprises the nervous signals to the muscles from the various oculomotor control centers in the brain. The output is the position of the globe relative to the orbit—the position of the line of sight relative to the head. This paper concentrates on the oculomotor plant and on models which mathematically represent its dynamics.

The oculomotor system has a number of functions. One involves positioning the globe so that the image of a given object falls on the fovea. If the object is moving, the brain may track it with the eye and use information from the oculomotor system to estimate motion parameters such as direction and velocity. By moving the eyes rather than moving the head the oculomotor system reduces the requirement for head movement.

3. Why model the oculomotor system?

An important motivation for oculomotor modelling is academic curiosity, as an understanding of the physiology of motor systems in general may be gleaned by studying the oculomotor system. It is unique among bodily motor systems in that, under natural conditions, it operates against a load (the moment of inertia of the globe) that is *constant* and *small* (when compared with the forces that the extraocular muscles generate). Since a number of techniques exist which allow the position of the eye to be measured with high spatial and temporal resolution, the oculomotor system is an accessible and attractive system to study. As when investigating any motor system, another objective is to gain an understanding of the strategies which the brain employs in generating particular movement patterns.

Oculomotor modelling may also be used in non-invasive studies of central nervous system (CNS) function. Since the inputs to a model may be the

innervations supplied by the CNS, measurement of eye position, in combination with ocular plant modelling, permits indirect 'observation' of CNS activity. Effects of drugs and disease processes on the CNS may then be observed in a quantitative and non-invasive manner. Normal functioning may also be observed with the goal of inferring the control strategies used by the brain in directing eye movements. Further, we may observe adaptation of the brain's control strategies in response to system perturbation, or unusual environmental conditions. Properties of neuromuscular transmission or properties of the muscles themselves can also be studied in this way.

4. Approaches to oculomotor modelling

Developing an accurate model of the oculomotor control system is an iterative process in which a model is empirically evaluated and then revised. To start the process one may use *a priori* knowledge of the system's structure and function. The interrelationship of the extraocular muscles, the globe and the orbital tissues is known from the relevant anatomy; knowledge of the dynamics of muscles and tissues may be derived from the study of their cell structures and composition and from studies of their biomechanics. One can trace the motor pathways which provide signals to drive the muscles and the sensory pathways which return information from the eye. Finally, our knowledge of system function can provide interpretation of observed behaviour.

One generally starts with a preliminary conceptualization of the system. Once a model has been constructed and implemented it is necessary to test its performance against measured system behaviour in order to verify its relevance and correctness. In dealing with the oculomotor system, measurement of eye position is not the only source of data; direct measurement of nerve-fibre activity and muscle activity (electromyographic recordings) may be used to provide information about system inputs. In collecting these data it is important to understand the effects of instrumentation error and other errors which may arise, because the system rarely operates under the exact conditions which the model presupposes.

In developing oculomotor models, there are two basic approaches. *Black-box* modelling deals only with input–output relationships and does not attempt to explain the internal workings of the system. *Homeomorphic* modelling, on the other hand, makes use of *a priori* information about the structure of the system in order to create models in which the system's inner workings are considered. The type of model employed depends on the intended use and on the level of one's understanding of the system's internal structure and function.

Black-box models are developed on the basis of empirical data concerning input–output relations (in this case nervous innervation to the muscles versus eye-position) and lead to representations of the system that say little about its internal workings. This provides a working description of system behaviour which in many cases is simpler than descriptions which attempt to account for internal processes. Sometimes these models are no more than exercises in curve fitting. Early oculomotor models were of this type.

One example is the empirical relationship between eye position $\theta(t)$, in degrees, and the firing rate of the oculomotor neurons $R(t)$ (expressed as the number of nerve impulses per second) proposed by Keller (1981) to be

$$R(t) = k\theta(t) + r\theta'(t) + m\theta''(t), \tag{1}$$

where k, r and m are constants. Performing a Laplace transform leads to a transfer function of the form

$$\frac{\theta(s)}{R(s)} = \frac{Kw_n^2}{s^2 + 2\Gamma w_n s + w_n^2}, \tag{2}$$

where $\theta(s)$ and $R(s)$ are understood to be the Laplace transforms of $\theta(t)$ and $R(t)$, respectively. The resulting transfer function is seen to be second-order, with w_n representing the 'natural frequency' of the solution and Γ the damping coefficient. This second-order transfer function had been proposed earlier by Westheimer (1954) as a result of observing that saccades resembled the step response of a second-order system. Saccades are high-velocity eye movements which serve to change the eyes' fixation from one point to another. They are of short duration, typically 30–70 ms, with duration increasing with increasing magnitude of movement. They can reach velocities of 1000 degrees per second of rotation (measured with respect to the orbit). An example of a relatively small saccade is shown in Figure 2.

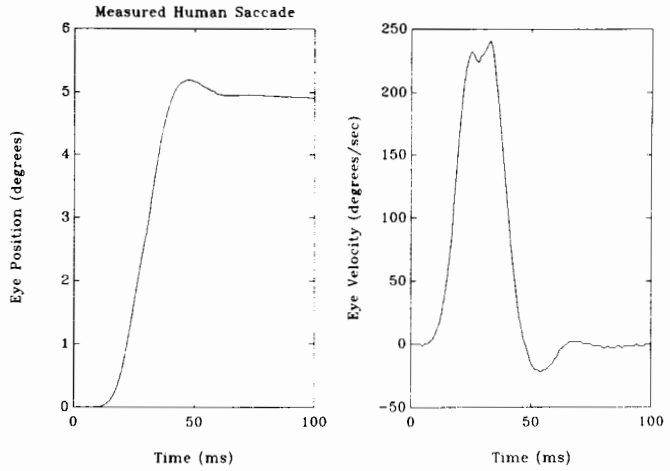

Figure 2. Human saccade. Eye displacement and velocity plotted against time for a saccade measured using a corneal reflection tracker developed by Frecker and Eizenman. (Frecker et al. (1983), Eizenman et al. (1984)).

The neural input which drives a saccade is thought to be a pulse followed by a step. A pulse-step consists of a short period in which the rate of neural discharge is very high, followed by a period at a lower discharge rate. The final rate is higher than the rate prior to the pulse, but not as high as during the pulse. The input $R(t)$ is the *difference* in the firing rates of the agonist and antagonist innervation signals. The term *agonist* refers to the muscle which is

contracting; *antagonist* refers to the muscle which is relaxing. This type of agonist–antagonist action is called *reciprocal innervation*.

An improvement to Westheimer's model was suggested by Robinson (1970) who noted that the input to the system during a saccade was not a step but rather a pulse-step. Robinson proposed a fourth-order model based on his empirical observations:

$$\frac{\theta(s)}{R(s)} = \frac{0.667(0.02s+1)}{(0.3s+1)(0.06s+1)(1.03\times10^{-5}s^2+0.004s+1)}. \tag{3}$$

This model generated more realistic saccadic trajectory profiles when compared with actual eye-movement data. However, the acceleration profiles predicted by the model were in poorer accord with the data. Both Westheimer's and Robinson's early models were linear transfer-function models of the black-box type. They offered limited insight into the internal structure and function of the oculomotor system.

An alternative to the black-box model is the homeomorphic model, in which each element corresponds to some known structure within the system. Homeomorphic models are conceptually satisfying in that, since each model element can be associated with some physical element of the original system, a better understanding of the internal workings of the system is obtained. The effect of varying individual parameters on model performance may be observed directly in the model's output.

The first linear homeomorphic model was proposed by Bahill in 1980. The model is shown in Figure 3 and the defining equations are given in (4). Parameter values are shown in Table 1. This model deals only with eye movements in the horizontal plane. The model consists of four basic elements: the agonist muscle, the antagonist muscle, the globe and the orbit. Each muscle is modelled as a force generator F in parallel with an elastic element K_{LT} and a viscous element B, and is connected to the globe through a series elastic element K_{SE}. The globe has a moment of inertia J_P and is connected to a visco-elastic element (consisting of K_P and B_P) which represents the orbital tissues. The agonist and antagonist act in direct opposition to each other and are innervated by separate neurological control signals N_{AG} and N_{ANT}; the input to each muscle is passed through a first-order filter with time constants T_{AG} and T_{ANT}, respectively.

One of the advantages of such a model is that it allows for separation of the signals controlling the muscles which form the agonist–antagonist pair for horizontal eye movements. This is desirable because the two muscles (lateral and medial rectus) are controlled by different areas in the brain stem (Zee and Lee (1983)). Also, it allows for different time constants for the two muscles. Since observed time constants are different for relaxing muscles and contracting muscles, and are also different for the agonist and antagonist (Bahill et al. (1980)) it is necessary to represent them separately. A comparison of the output of this model with an observed human saccade, measured in the authors' laboratory, is shown in Figure 4.

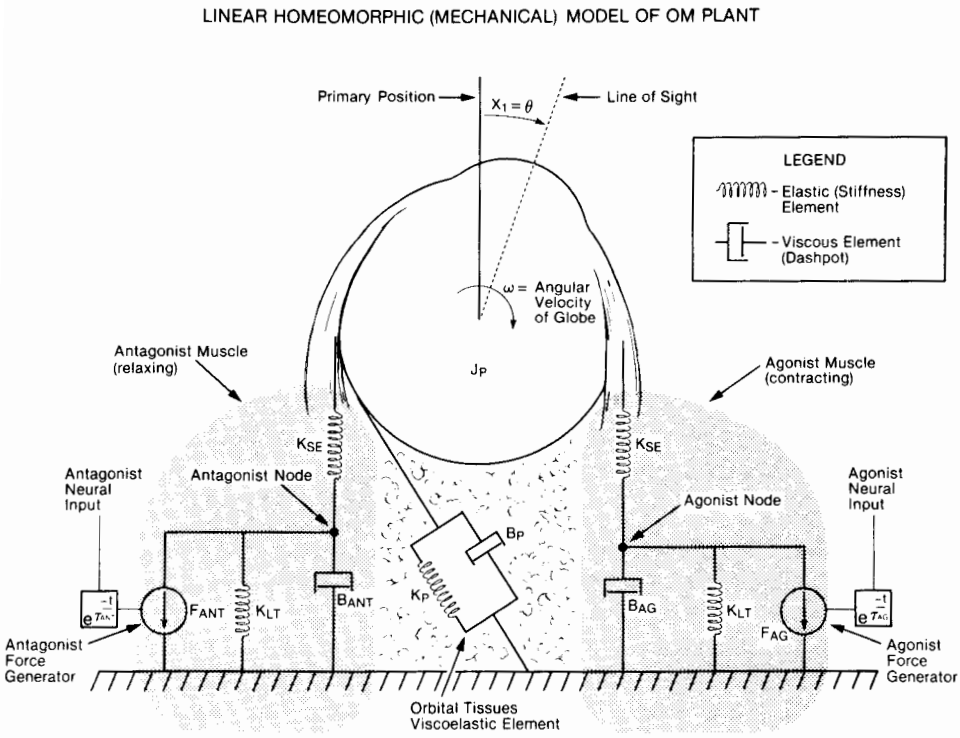

Figure 3. Linear homeomorphic model. A mechanical reciprocal innervation model for eye movements (for horizontal movements the agonist–antagonist pair are the lateral and medial recti; see Figure 1). This is the plant model proposed by Bahill et al. (1983).

Table 1. Parameter values for a sixth-order linear homeomorphic model. The parameters are for Bahill's sixth-order linear homeomorphic model. Note that the time constant for the accelerating agonist ($\tau_{AG\text{-}AC}$) is dependent on the magnitude of the eye movement. This reflects that this time constant models the fact that higher rates of neuronal discharge, associated with larger movements, develop tension more quickly than lower rates and therefore should be associated with a smaller time constant. See text for definitions.

K_{SE}	2.5 g tension/°	J	4.3×10^{-5} g s^2/°
K_{LT}	1.2 g/°		
K_P	0.5 g/°	$\tau_{AG\text{-}AC}$	$(11.7-0.2\delta\theta)$ ms
B_P	0.06 g s/°	$\tau_{AG\text{-}DE}$	0.2 ms
B_{AG}	0.046 g s/°	$\tau_{ANT\text{-}AC}$	2.4 ms
B_{ANT}	0.022 g s/°	$\tau_{ANT\text{-}DE}$	1.9 ms

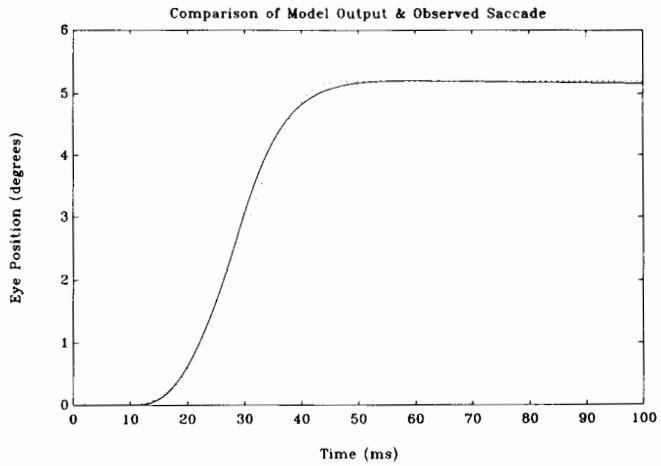

Figure 4. Observed saccade versus model output. The saccade shown in Figure 2 is compared with model output. The measured saccade overshoots slightly.

In the system equations, the state variables were chosen to be eye position, eye velocity, position of the agonist and antagonist nodes (the point where K_{SE} joins the force generator, Figure 3) and the developed tension between the agonist and the antagonist. A different choice of variables for the same system might lead to a different but equivalent model. In fact, Enderle and Wolfe (1984), (1987) chose eye position, velocity, acceleration, and jerk (rate of change of acceleration) as the first four state variables in their more recent model (Equation (4a)). The behaviour of the model is similar, as will be discussed below. A set of six differential equations written in terms of the state variables describes the system. These may be written in matrix form (as in Equation (4)) and state-space methods may be used to solve the system explicitly for certain cases.

5. Mathematical tools available

5.1. *Time and frequency domain analysis.* Systems-control theory is the basis for quantitative study of a wide variety of mechanical, electrical, chemical and biological systems. It often simplifies analysis by replacing differential equations in the time domain with algebraic equations in the complex frequency domain (as in Equations (2) and (3)). Solution for the transfer function of the system is then reduced to algebraic manipulations of these equations. An example of the use of systems control theory is Van Opstal et al.'s (1985) reconstruction of neural control signals from measured eye movement trajectories. By observing the output (eye position) during any type of eye movement (e.g., a saccade) and by adopting a model, one can reconstruct the neural control inputs that would be necessary to generate the observed output. Using this method, Van Opstal et al. demonstrated the change in neural control signals associated with the administration of a tranquilizing drug (diazepam). The normal and perturbed signals are shown in Figure 5.

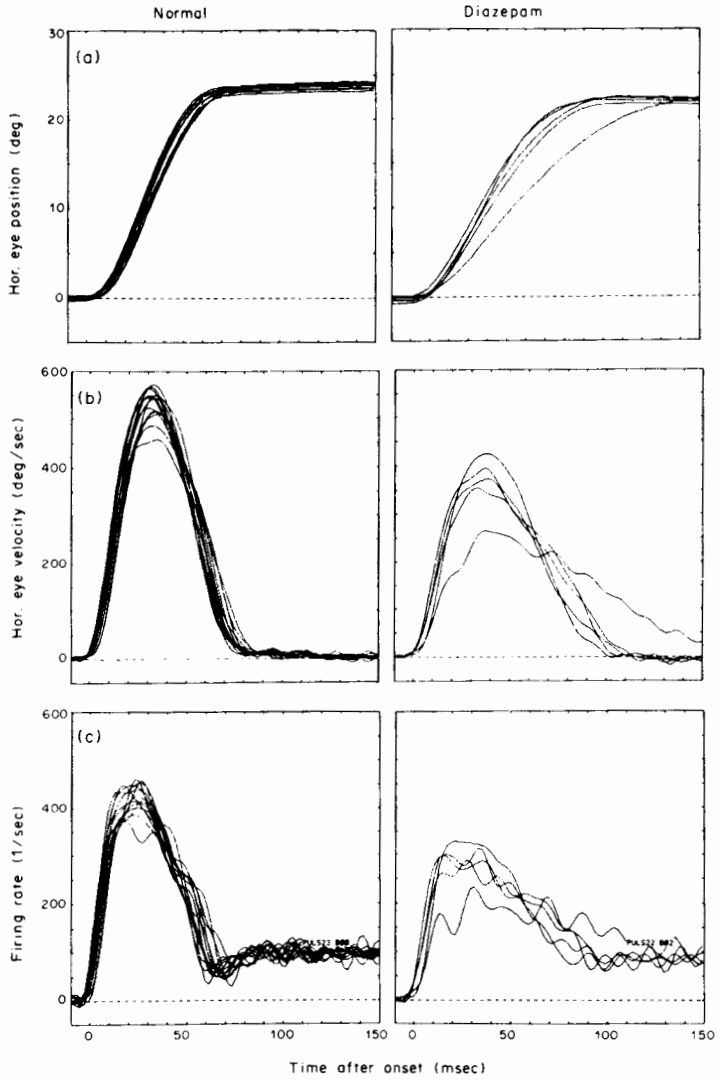

Figure 5. Reconstruction of neural signals by inverse method. Reconstructed pulse-step signals for normal and diazepam saccades. (a) Position signals, (b) computed horizontal velocity profiles and (c) reconstructed neural control signals for 13 normal saccades with amplitude between 23° and 24° (left-hand column) and 5 saccades with amplitude between 22° and 23° made after an intravenous injection of 7 mg diazepam (right-hand column). Time scale from 10 ms before to 150 ms after detected saccade onset. The diazepam saccades are much slower and have longer durations than normal saccades. Velocity profiles and neural control signals are more skewed in the diazepam saccades and the dip, which appears in the reconstructed input signal for normal saccades, is absent. Reprinted with permission of Pergamon Journals.

Homeomorphic model (Bahill et al. (1980))

$\dot{\boldsymbol{x}} = A\boldsymbol{x} + \boldsymbol{f}$, that is,

$$\begin{bmatrix} \dot{x}_1 \\ \dot{x}_2 \\ \dot{x}_3 \\ \dot{x}_4 \\ \dot{x}_5 \\ \dot{x}_6 \end{bmatrix} = \begin{bmatrix} 0 & 0 & 0 & 1 & 0 & 0 \\ \dfrac{K_{SE}^2}{(K_{LT}+K_{SE})B_{AG}} & -\dfrac{K_{SE}}{B_{AG}} & 0 & 0 & \dfrac{K_{SE}}{(K_{LT}+K_{SE})B_{AG}} & 0 \\ \dfrac{K_{SE}^2}{(K_{LT}+K_{SE})B_{ANT}} & 0 & -\dfrac{K_{SE}}{B_{ANT}} & 0 & 0 & \dfrac{K_{SE}}{(K_{LT}+K_{SE})B_{ANT}} \\ -\dfrac{2K_{SE}-K_P}{J_P} & \dfrac{K_{SE}}{J_P} & \dfrac{K_{SE}}{J_P} & -\dfrac{B_P}{J_P} & 0 & 0 \\ 0 & 0 & 0 & 0 & -\dfrac{1}{\tau_{AG}} & 0 \\ 0 & 0 & 0 & 0 & 0 & -\dfrac{1}{\tau_{ANT}} \end{bmatrix} \begin{bmatrix} x_1 \\ x_2 \\ x_3 \\ x_4 \\ x_5 \\ x_6 \end{bmatrix} + \begin{bmatrix} 0 \\ 0 \\ 0 \\ 0 \\ \dfrac{N_{AG}}{\tau_{AG}} \\ \dfrac{N_{ANT}}{\tau_{ANT}} \end{bmatrix}, \quad (4a)$$

where x_1 denotes the position of the eye, x_2 the position of the agonist node (see Figure 3), x_3 the position of the antagonist node, x_4 the velocity of the eye, x_5 the agonist active-state tension and x_6 the antagonist active-state tension.

Linear homeomorphic model (Enderle and Wolfe (1984))

$\dot{\boldsymbol{x}} = A\boldsymbol{x} + B\boldsymbol{u}$, that is,

$$\begin{bmatrix} \dot{x}_1 \\ \dot{x}_2 \\ \dot{x}_3 \\ \dot{x}_4 \\ \dot{x}_5 \\ \dot{x}_6 \end{bmatrix} = \begin{bmatrix} 0 & 1 & 0 & 0 & 0 & 0 \\ 0 & 0 & 1 & 0 & 0 & 0 \\ 0 & 0 & 0 & 1 & 0 & 0 \\ -P_0 & -P_1 & -P_2 & -P_3 & \dfrac{\delta(K_{ST}-B_{ANT})}{\tau_{AG}} & -\dfrac{\delta(K_{ST}-B_{AG})}{\tau_{ANT}} \\ 0 & 0 & 0 & 0 & -\dfrac{1}{\tau_{AG}} & 0 \\ 0 & 0 & 0 & 0 & 0 & -\dfrac{1}{\tau_{ANT}} \end{bmatrix} \begin{bmatrix} x_1 \\ x_2 \\ x_3 \\ x_4 \\ x_5 \\ x_6 \end{bmatrix} + \begin{bmatrix} 0 & 0 \\ 0 & 0 \\ 0 & 0 \\ \dfrac{\delta B_{ANT}}{\tau_{AG}} & -\dfrac{\delta B_{AG}}{\tau_{ANT}} \\ \dfrac{1}{\tau_{AG}} & 0 \\ 0 & \dfrac{1}{\tau_{ANT}} \end{bmatrix} \begin{bmatrix} N_{AG} \\ N_{ANT} \end{bmatrix}, \quad (4b)$$

where x_1 denotes the position of the eye, x_2 the velocity of the eye, x_3 the acceleration of the eye, x_4 the jerk of the eye, x_5 the agonist active-state tension and x_6 the antagonist active-state tension.

It is also possible to work directly in the time domain. An nth-order differential equation may be written as n first-order differential equations of n variables, in matrix form (see Equations (4a) and (4b), pp. 144 and 145). The n variables are referred to as state variables and the resulting equation as a state-space equation. State-space methods are useful regardless of which model is chosen. The second- and fourth-order models, presented previously as transfer-function models (Equations (2) and (3)), may easily be rewritten in state-space form. The Bahill and Enderle models are already in this form. The general form for a state-space equation may be given as

$$\dot{\boldsymbol{x}}(t) = A(t)\boldsymbol{x}(t) + \boldsymbol{u}(t) + \boldsymbol{e}(t), \tag{5}$$

where $\boldsymbol{x}$ is an $n\times 1$ column vector, A is an $n\times n$ matrix, and $\boldsymbol{u}$ and $\boldsymbol{e}$ are $n\times 1$ column vectors. The vector $\boldsymbol{u}$ is the system input (or forcing function) and $\boldsymbol{e}$ is a stochastic process (noise function). For the homeomorphic models given above, the noise function is ignored and the A matrix is stepwise constant (i.e., it is constant within a given time period and only changes at discrete points in time). We can solve Equation (5) explicitly for an interval $\tau = [t_0, t_1]$ if it is known that $\boldsymbol{u}$ and $A(t)$ are continuous on τ. We can then write a solution as

$$\boldsymbol{x}(t) = \Phi(t, t_0)x_0 + \int_{t_0}^{t} \Phi(t, s)\boldsymbol{u}(s)\, \mathrm{d}s, \tag{6}$$

where

$$\Phi(t, t_0) = \sum_{k=0}^{\infty} \frac{A^k(t-t_0)^k}{k!} = \exp A(t-t_0) \tag{7}$$

and $\boldsymbol{x}_0 = \boldsymbol{x}(t_0)$.

If A and $\boldsymbol{u}$ are stepwise constant, then the solution of Equation (6) is relatively straightforward. One case where $\boldsymbol{u}$ is stepwise constant occurs when the input is a pulse-step which is the innervation signal used to generate a saccade. The explicit solution for this is given by

$$\boldsymbol{x} = [\exp A(t-t_0) - I]A^{-1}\boldsymbol{u} + \exp A(t-t_0)\, \boldsymbol{x}(t_0), \tag{8}$$

where I is the $n\times n$ identity matrix. The solution is valid over the time interval $[t_0, t_1]$ in which A and $\boldsymbol{u}$ are constant. It has two parts: a particular solution which depends on the value of the state at the beginning of the interval and a solution to the homogenous equation which is an exponential function of the state matrix A. For the solution to be stable the eigenvalues of A must all have negative real parts, since otherwise the exponential will grow without bound. $\exp At = P\exp(\Lambda t)P^{-1}$, where Λ is a diagonal matrix whose elements are the eigenvalues of A and $A = P\Lambda P^{-1}$. This also provides a computationally efficient way of evaluating $\exp At$ if it is diagonalizable.

In order for this model to be useful, one needs to assign parameter values to the A and B matrices. This, in general, is a problem in system identification. For the homeomorphic model, many of the parameters may be difficult or impossible to measure experimentally. Further, parameters are likely to vary

from one individual to another, and vary with time for a given individual. Therefore, it is desirable to be able to identify the values of the parameters, using observations of the system, or through having prior knowledge of the range in which the parameter values might lie.

5.2. *Parameter identification.* Parameter-identification techniques generally work by minimizing a cost or error function with respect to the parameter values. Since we do not know the true parameter values, this cost function is written in terms of the system and model responses (Bekey (1976)). In Figure 6 we see the comparison of the measured output $y(t)$ and the model output $z(t)$ for the same input sequence.

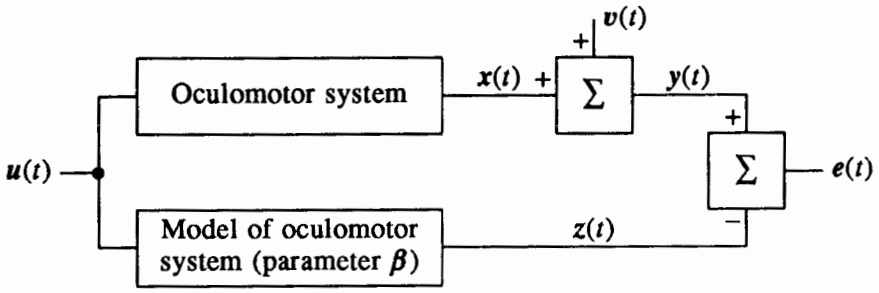

Figure 6. System identification. Schematic representation of parameter identification using system and model.

The output value $y(t)$ is corrupted by measurement errors or noise $v(t)$. Since the model depends on the parameters β, we can write $z(t) = z(t,\beta)$. We define the error to be $e(t,\beta) = y(t) - z(t,\beta)$ and choose the error criterion to be the least-squares error criterion.

$$J(\beta) = \int_{t_0}^{t_1} e(t,\beta)^{\top} e(t,\beta)\, \mathrm{d}t. \tag{9}$$

Other error criteria are available, but the least-squares criterion is well studied and in some cases is optimal, depending on noise characteristics. By minimizing J with respect to β we can choose values for the parameters β. If the second-order statistics of v are known ($R = E[v^{\top} v]$ is known) or can be estimated, an improved criterion (weighted least-squares error) is given by

$$J(\beta) = \int_{t_0}^{t_1} e(t,\beta)^{\top} R^{-1} e(t,\beta)\, \mathrm{d}t. \tag{9a}$$

There are many algorithms for minimizing $J(\beta)$ and many relevant 'off-the-shelf' software packages. One of the more popular methods is the method of steepest descents. This method makes use of the fact that $J(\beta)$ is a surface in n-space (called the error-performance surface) which will have at least a local minimum. Starting with an initial guess $\beta^{(0)}$ we can estimate $\beta^{(i+1)}$ as follows:

$$\beta^{(i+1)} = \beta^{(i)} - K \operatorname{grad} J(\beta^{(i)}). \tag{10}$$

Starting with $\beta^{(0)}$, this method attempts to find the bottom of the error-performance surface, which is the point of minimum error, by travelling along the maximum gradient. The constant K is a step-size parameter on which the stability and speed of convergence is dependent. When, and if, $\beta^{(i)}$ converges to a stable value, one has found an optimal β for the model. Given the relatively low cost of computer time and the popularity of state-space methods, this is currently a popular technique. Other methods include Newton–Raphson methods, random searches and transfer-function identification (Bekey and Yamashiro (1976)).

5.3. *Parameter sensitivity.* In identifying parameter values which result in optimal model performance, it is instructive to have a measure of the sensitivity of model behaviour to changes in each parameter. The sensitivity of output state x_i to a change in parameter β_j may be written as

$$S_{ij} = \frac{\delta x_i}{\delta \beta_j}, \tag{11}$$

or, in relative terms, as

$$\bar{S}_{ij} = \left[\frac{\delta x_i}{\delta \beta_j} \frac{\beta_j}{x_i} \right]_{\beta_j}.$$

This helps to identify which parameters, when changed by a small amount, will cause a large change in model behaviour. Such parameters are important to identify so that their values may be estimated with the greatest accuracy. Sensitivity analysis aids in refining model structure by showing which elements are relatively important or unimportant, warning of unusual model behaviour and evaluating model validity (Bahill (1980)). (Table 2 gives a partial ranking of the sensitivity of parameters in Bahill's homeomorphic model.)

Table 2. Rank of parameter sensitivities in the sixth-order linear homeomorphic model.

$K_{\text{AG-LT}}$	1	B_{ANT}	8
$K_{\text{AG-SE}}$	2	$K_{\text{ANT-LT}}$	9
B_{P}	3	$\tau_{\text{ANT-DE}}$	10
B_{AG}	4	J	11
$\tau_{\text{AG-AC}}$	5	$\tau_{\text{ANT-AC}}$	12
$K_{\text{ANT-SE}}$	6	$\tau_{\text{AG-DE}}$	13
K_{P}	7		

5.4. *Time-optimal control.* It was noted in the introduction that observation of the oculomotor system could be used to infer control strategies used by the brain in controlling eye movements. One such strategy currently being investigated in our laboratory is that of time optimality. A time-optimal strategy implies that saccadic eye movements are carried out in such a manner as to minimize the duration of the movement and, subsequently, the disruption of the flow of visual information to the brain. Such a strategy could be argued in evolutionary terms on the basis of increased survival capacity resulting from

minimized visual disruption during saccades. Several authors, notably Clark and Stark (1975), Lehman and Stark (1983) and Enderle and Wolfe (1987) have investigated this concept using both linear and non-linear models. Their results suggest that the eye may be controlled during saccades by an on-off multi-pulse signal. By combinations of pulses, in which innervations to the muscles are turned full-on or full-off, the eye may be moved to its new position in minimum time. A mathematical definition of time optimal control (Enderle and Wolfe (1987)) might be the requirement that the eye movement trajectory $\theta(t)$ must minimize the function

$$J(\boldsymbol{u}) = \int_0^{t_f} \mathrm{d}t + [\theta(t_f) - \boldsymbol{D}]^\top G[\theta(t_f) - \boldsymbol{D}] = t_f + [\theta(t_f) - \boldsymbol{D}]^\top G[\theta(t_f) - \boldsymbol{D}] \quad (12)$$

with respect to $\boldsymbol{u}$, the neural-signal responsible for the motion. Here G is a weighting matrix, $\boldsymbol{D}$ is the desired final state (or destination) of the system, $\theta(t)$ is the state of the system at time t and t_f is the terminal time. $J(\boldsymbol{u})$ therefore takes into account the time to reach the final position as well as the error in the final position from the desired final position. The resulting value of $\boldsymbol{u}$ would be the optimal control signal. A result of minimizing is that at any time, $\boldsymbol{u}$ is at its maximum or minimum value (a bang-bang controller) (Enderle and Wolfe (1987)).

6. Model evaluation

Knowledge of the physiological signals which actually drive the extraocular muscles is prerequisite to adequate model evaluation. While recordings from single nerve cells during a saccade have been shown to resemble a pulse-step, the relevant input to the model is the sum of activity from all active nerve cells. It is unlikely that all cells fire with precise synchrony or that their duration of firing is the same. Also, many measured saccades overshoot their target and are thought to be corrected by a reversal pulse. The physiological existence of such a corrective pulse is unproven.

Nonetheless, a variety of empirical approaches to model evaluation have been used. One approach is to sum the squared error between the position estimates from the model and the measured eye position. Bahill (1980) compared the second-, fourth- and sixth-order models for a 10-degree saccade in this manner and found that the sixth-order model performed best, with a total error of 49×10^{-6} degrees^2. The second-order model was 3- to 46-fold less accurate, depending on how it was conceived. Greater accuracy was obtained with an underdamped second-order system and a step input; less accuracy was obtained with an overdamped system and a pulse-step input. The latter, however, appears to be more realistic in terms of known physiological and mechanical input and plant parameters. The sixth-order model also produced acceleration profiles that more closely matched observed profiles than did the second-order model, suggesting overall a more accurate description of oculomotor behaviour.

The parameters of the sixth-order model used to generate the plot in Figure 4 were not tailored to the particular measured saccade. In fact, parameter values obtained from the literature were used. That a close correspondence was

obtained suggests a degree of model robustness. However, a sixth-order model is undeniably more difficult to work with than a second-order model, and certain uses may not justify the extra computational effort.

7. Future approaches

In what direction should new efforts towards oculomotor modelling move? What does one hope to gain through such efforts? First is the development and testing of better oculomotor models. For models to be useful in the long term they must be subjected regularly to scrutiny, revision and validation through empirical testing.

With improved models a variety of processes might be investigated. The study of control strategies appears important, with particular attention to the manner in which adaptation takes place. Study of cerebellar anatomy suggests the existence of structures with adaptive properties (Grossberg (1986)). These may be involved in adaptation to new external and internal (physiological) conditions and in the learning of fine motor responses. Quantitative measurement of adaptation processes should help to identify the adaptive structures and the relevant parameters.

Neurophysiological processes that affect muscle performance may be probed by studying the effect of time on model parameters. This would be facilitated through the development of algorithms which track model parameters continuously, a problem closely related to that of adaptive filtering. Such studies, when linked to known neurotransmitter mechanisms, may also lead to a better understanding of the effects of drugs on human performance and perception.

Finally, modelling may help satisfy our curiosity about the functioning of human motor systems. Motion is an important aspect of daily functioning, and it is helpful to understand the brain's control of motion in order to better understand the brain itself.

References

BAHILL, A. T. (1980) Development, validation and sensitivity analyses of human eye movement models. *CRC Crit. Revs. Bioeng.* (Dec) 311–355.

BAHILL, A. T., LATIMER, J. R. AND TROOST, B. T. (1980) Linear homeomorphic model for human movement. *IEEE Trans. Biomed. Eng.* **27**, 631–639.

BEKEY, G. A. AND YAMASHIRO, S. M. (1976) Parameter estimation in mathematical models of biological systems. In *Advances in Biomedical Engineering*, ed. J. H. U. Brown and J. F. Dickson. Academic Press, New York, 1–43.

CARPENTER, R. H. S. (1977) *Movements of the Eyes.* Pion, London.

CLARK, M. R. AND STARK, L. (1975) Time optimal behavior of human saccadic eye movement. *IEEE Trans. Automat. Contr.* **20**, 345–348.

DAVSON, H. (1980) *Physiology of the Eye.* Academic Press, New York.

EIZENMAN, M., FRECKER, R. C. AND HALLETT, P. E. (1984) Precise non-contacting measurements of eye movements using the corneal reflex. *Vision Res.* **24**, 167–174.

EYKHOFF, P. (1974) *Systems Identification.* Wiley, New York.

ENDERLE, J. D., WOLFE, J. W. AND YATES, J. T. (1984) The linear homeomorphic saccadic eye movement model—a modification. *IEEE Trans. Biomed. Eng.* **31**, 717–720.

ENDERLE, J. D. AND WOLFE, J. W. (1987) Time-optimal control of saccadic eye movements. *IEEE Trans. Biomed. Eng.* **34**, 43–55.

FRECKER, R. C., EIZENMAN, M. AND HALLETT, P. E. (1984) High-precision real-time measurement of eye position using the first Purkinje image. In *Theoretical and Applied Aspects of Eye Movement Research*, ed. A. G. Gale and F. Johnson. North-Holland, Amsterdam, 13–20.

GROSSBERG, S. (1986) Adaptive compensation to changes in the oculomotor plant. In *Adaptive Processes in Visual and Oculomotor Systems*, ed. E. L. Keller and D. S. Zee. Pergamon Press, Oxford, 341–345.

KELLER, E. L. (1981) Oculomotor neuron behavior. In *Models of Oculomotor Behavior and Control*, ed. B. L. Zuber. CRC Press, Boca Raton, Fl.

LEE, E. B. (1960) Mathematical aspects of the synthesis of linear minimum response-time controllers. *IRE Trans. Automat. Contr.* **5**, 283–289.

LEHMAN, S. L. AND STARK, L. W. (1983) Multi-pulse controller signals—II: Time optimality. *Biol. Cybernet.* **48**, 5–8.

LEIGH, R. J. AND ZEE, D. S. (1983) *The Neurology of Eye Movement*. F. A. Davis, Philadelphia.

ROBINSON, D. A. (1970) Oculomotor unit behavior in the monkey. *J. Neurophysiol.* **33**, 393.

ROBINSON, D. A. (1981) Models of the mechanics of eye movements. In *Models of Oculomotor Behavior and Control*, ed. B. L. Zuber. CRC Press, Boca Raton, Fl.

SMITH, F. W. (1961) Time-optimal control of higher-order systems. *IRE Trans. Automat. Contr.* **6**, 16–21.

VAN OPSTAL, A. J., VAN GISBERGEN, J. A. M. AND EGGERMONT, J. J. (1985) Reconstruction of neural control signals for saccades based on an inverse method. *Vision Research* **25**, 789–801.

WESTHEIMER, G. (1954) Mechanism of saccadic eye movements. *AMA Arch. Ophthal.* **52**, 710–724.

YOUNG, L. R. AND SHEENA, D. (1975) Methods and designs: Survey of eye-movement recording methods. *Behav. Res. Meth. Instr.* **7**, 397–429.